

A Multivariate Statistical Analysis of Spiral Galaxy Luminosities. II. Morphology-Dependent Multiwavelength Emission Properties

G. Fabbiano

Harvard-Smithsonian Center for Astrophysics,
60 Garden Street, Cambridge, MA 02138

Alice Shapley

California Institute of Technology,
Pasadena CA, 91125, USA

ABSTRACT

This is the second of two papers based on a systematic multi-wavelength (X, B, H, $12\mu\text{m}$, FIR, 6cm) statistical analysis of the *Einstein Observatory Galaxy Catalog* sample of 234 ‘normal’ S0/a-Irr galaxies. This sample is representative of spiral galaxies (Paper I), and its wide wavelength coverage provides a unique opportunity for a systematic exploration of the relations among different emission bands, that can give novel insight on the different emission processes and their relation to galaxian components, as a function of galaxy morphology.

We find clear morphological differences in the overall relationships among different emission bands: while all wave-bands tend to be well correlated in late-type Sc-Irr galaxies, in agreement with a general connection of all emission bands with the stellar component, in bulge-dominant early-type S0/a-Sab galaxies, instead, our results point to unrelated emission mechanisms for the two groups of wave-bands ($12\mu\text{m}$, FIR, 6cm) and (X, B, H).

A dependence on galaxy morphology is also found in the $12\mu\text{m}$ – FIR link, which was shown by the multivariate analysis of Paper I to be one the two strongest fundamental correlations in spiral galaxies, together with the well-known B – H correlation. We find that blue late-type dwarf galaxies appear to lack $12\mu\text{m}$ emission, suggesting a lack of small-size dust grains in their ISM, perhaps resulting from a particularly intense UV photon field. Also, the IR – B color-color plot of S0/a-Sab galaxies presents more scatter than those of later-type galaxies, suggesting both significant red giant circumstellar dust emission and nuclear emission.

Examining the well-known IR – radio continuum link of spiral galaxies, we find surprising morphological differences: the ‘fundamental’ radio-IR correlation flips from the mid-IR ($12\mu\text{m}$) emission in S0/a-Sab galaxies, to the FIR in Sc-Irr. These correlations also have different slopes: the 6cm – $12\mu\text{m}$ correlation of S0/a-Sab galaxies is steep and follows the same trend as that of the bright AGNs in the sample, suggesting that low-luminosity AGN embedded in these ‘normal’ galaxies may be

responsible for the bulk of their mid-IR and radio emission; the 6cm – FIR correlation of Sc-Irr galaxies is linear, consistent with the well known star-formation link.

The X-ray emission is not strongly correlated with any of the other variables, with the exception of the FIR in Sc-Irr, consistent with a general link with the young stellar population in these systems. Contrary to preliminary reports, we find that the X-ray – B correlation is similarly non-linear (slope ~ 1.5) in early- and late-type spirals. We suggest that this apparent similarity stems from different processes in the two samples. In S0/a-Sab's the steep slope may be due to the presence of some hot ISM in the more X-ray luminous systems, as observed in E and S0 galaxies. In Sc-Irr galaxies instead it may be related to a luminosity-dependence of intrinsically absorbed X-ray emission regions, connected with star formation activity. Obscured star-forming regions in higher luminosity galaxies can also explain other functional relations of the correlations found in the Sc-Irr sample.

Subject headings: galaxies: spiral — X-rays: galaxies

1. Introduction

Understanding the structure, formation and evolution of galaxies is one of the main themes of present-day astrophysics. This quest is made difficult by the complexity of galaxies combined with our limited knowledge of their observational characteristics. Different galaxian components [old, new, evolved stars; active nuclei (AGN); the interstellar medium (ISM) – gaseous; dusty; hot; cold] contribute in different amounts to the observed emission at different wavelengths, from the radio to the X-rays (see Gallagher & Fabbiano 1990). Therefore the comparison of global emission properties in a wide range of wavelengths can give us precious insight on the relative importance of these components, as well as on the origin of some parts of the emission spectrum. Since different emission bands have different sensitivities to absorption, their comparison may also give us insight on the dust content of the emitting regions (e.g. Palumbo et al. 1985; Fabbiano & Trinchieri 1987). Moreover, comparison of global multiwavelength emission properties of galaxies of different morphology can give us insight on the relative presence of different galaxian components throughout the Hubble sequence.

While most of the studies of galaxies make use of individual energy bands, chiefly the optical, but also the radio, and more recently the X-ray and infrared (IR), it is rarer to find work comparing data from two or more emission windows. Yet, when this is done interesting insights may follow. For example, the comparison of H-band and B-band photometry led to the discovery of the well known color-magnitude relation for spiral galaxies (Aaronson, Huchra & Mould 1979; Tully, Mould & Aaronson 1982), a non-linear correlation between L_B and L_H . The comparison of IRAS far-IR and radio continuum data led to the discovery of the well-known strong correlation and to the convincing association of the radio continuum emission with the star-forming stellar

population (Dickey & Salpeter 1984; Helou, Soifer & Rowan-Robinson 1985; de Jong et al. 1985); comparison of CO, H α and IR data led to constraints on star formation efficiencies in spirals (e. g. Young 1990); comparison of multiwavelength data, including X-rays, in late-type spirals suggested the prevalence of intrinsically obscured compact star-forming regions in higher luminosity galaxies (Fabbiano, Gioia & Trinchieri 1988; Trinchieri, Fabbiano & Bandiera, 1989).

This paper is a panchromatic study of a sample of 234 normal galaxies extracted from the *Einstein Observatory Atlas and Catalog of Galaxies* (Fabbiano, Kim & Trinchieri 1992, hereafter FKT). The sample is large enough to divide into morphological sub-samples. Details on the sample selection and properties, and on the compilation of the multi-frequency data are given in Paper I (Shapley, Fabbiano & Eskridge 2001), together with a description of the statistical analysis of these data. Here we examine the astrophysical import of the results of Paper I, and we support these results with further analysis. We take the panchromatic approach by comparing the global emission properties of spiral and irregular galaxies in six emission windows: X-rays (0.2-4 keV), optical (B), near- (H), mid- ($12\mu\text{m}$) and far-infrared (60-100 μm , FIR), and radio continuum (6cm). We also take into account explicitly the morphological type of the galaxies, by dividing the sample in early (S0/a-Sab), intermediate (Sb-Sbc) and late (Sc-Irr) subsamples, and intercomparing the luminosity correlations in the three subsamples.

Previous panchromatic explorative work including the X-ray band was based on a much smaller sample of 51 spirals observed in X-rays with the *Einstein Observatory* (Fabbiano & Trinchieri 1985, hereafter FT; Fabbiano, Gioia & Trinchieri 1988 hereafter FGT; see Fabbiano 1990). This earlier work suggested interesting results and motivated the present effort. Differences were reported in both scatter and power-law ‘slopes’ of the correlations, when comparing bulge-dominated and disk/arm-dominated spirals, pointing to different contributions of bulge and disk to the various emission bands. In late-type spirals, all the correlations appeared to be very tight, but with different power-law slopes. Departures from linearity suggested the prevalence of intrinsically obscured compact star-forming regions in higher luminosity galaxies. Based on the analysis of a yet smaller sample of 17 late-type spirals, the puzzling possibility was advanced of an intrinsic link between X-ray sources and cosmic ray sources responsible for the radio non-thermal continuum (FT, FGT). This radio – X-ray link seems at odds with the prevalent association of radio continuum and the FIR-emitting star-forming component (e.g. Helou, Soifer & Rowan-Robinson 1985).

Some of the above reports may stem from limited statistics. Others may point to intrinsically complex astrophysical situations. Our present sample, being nearly five times larger than the one used in previous work, gives us an opportunity to look at some of these issues afresh with the benefit of a much stronger statistical foundation. Moreover, this sample comprises 58 S0/a-Sab galaxies, versus the 16 that were included in the FT and FTG works. Furthermore, the inclusion of the $12\mu\text{m}$ band in the present analysis allows for a more complete wavelength coverage than in previous work. It therefore allows us for the first time to study the average emission properties of early-type spirals with a reasonable degree of confidence.

This paper is organized as follows: after the Introduction (§1.), §2. summarizes the characteristics of the sample and the analysis methods used in Paper I; §3. discusses the evidence linking some emission bands prevalently to the disk/arm component and others to the bulge component as well; §4. and §5. discuss morphology-related differences in the mid-, far-infrared, and radio continuum emission, and their implication for our understanding of the radio continuum and mid-IR emission of S0/a-Sab galaxies; §6. discusses the X-ray – B correlation and the implications of our results for the origin of the X-ray emission of bulge-dominant S0/a-Sab galaxies; §7. discusses the link of the X-ray emission of late-type spirals with the star-forming stellar population, and §8. addresses the non-linear power-law dependencies in disk/arm dominated galaxies; §9. summarizes the results.

2. The Sample and Data Analysis

The sample and data analysis procedures are fully described in Paper I. The sample (extracted from FKT) consists of 234 ‘normal’ spiral and irregular galaxies (from S0/a to Irr) observed in (0.2-4)keV X-rays with the *Einstein Observatory*. The FKT sample included also 21 bright Active Galactic Nuclei (AGN), where the X-ray emission is clearly dominated by the nuclear source. We do not use these galaxies in our analysis unless explicitly stated. As discussed in Paper I, the FKT sample selection is optical and reflects the basic incompleteness of the RC2. Since the sample is not statistically complete, nor X-ray selected, it cannot be used to infer directly the X-ray luminosity function of spiral galaxies. However, the FKT sample offers a fair representation of spiral galaxies, with good coverage in both morphological types and luminosity range, and it does not suffer from peculiar distance biases (Paper I). It is therefore a good representative sample for studying average emission properties. This sample represents nearly a five-fold increase by comparison with previous statistical analyses of late-type galaxies observed in X-rays (FT; FGT).

As discussed in Paper I, multiwavelength fluxes were obtained through literature searches, and converted to luminosities for our analysis, using the distances listed and discussed in Paper I. The bands covered include, besides the X-rays, the optical B, near-IR $1.6\mu\text{m}$ H, IRAS $12\mu\text{m}$ and FIR (plus individual use in some cases of the $60\mu\text{m}$ and $100\mu\text{m}$ data), and 6cm radio continuum. The inclusion of 6cm, instead of 20cm, as an indicator of radio continuum allows us to compare directly the results of the spiral sample with those of E and S0s (Eskridge, Fabbiano & Kim 1995, hereafter EFK). In all cases, both detections and upper limits were included, to avoid obvious flux limit biases in the non-optical bands.

The data were analysed using the censored statistical analysis package ASURV (e.g., Isobe, Feigelson & Nelson 1986; LaValley, Isobe & Feigelson 1992), and custom multivariate statistical software developed by our group (Paper I). We tested all possible pairs of luminosity variables for statistically significant correlations, and also compared several illustrative sets of flux ratios. We then performed regression analysis on the luminosity correlations and derived regression ‘bisectors’ representing the functional relations between any given pair of variables. To discriminate between

intrinsically strong correlations, and correlations that may be the by-product of other stronger links, we performed a multivariate conditional probability analysis using the Partial Spearman Rank method (Kendall & Stuart 1976; see FGT and EFK for previous applications). The use of both detections and limits in the analysis, and the sample selection criteria should protect us from distance biases. However, we also included explicitly the distance in our multivariate analysis, thus confirming that the correlations between luminosities are not a spurious distance effect (see Paper I).

We analysed both the sample as a whole and three subsamples including galaxies of different morphological types: the early sample (58 T=0-2 S0/a-Sab galaxies; we excluded from this subsample 7 Amorphous galaxies with T=0, see Paper I) including galaxies with prominent bulges; the intermediate sample (61 galaxies; T=3-4; Sb-Sbc), typically consisting of luminous bulge/disk spirals; and the late sample (108 galaxies; T=5-10; Sc-Irr), which includes galaxies dominated by the disk/arm star-forming component.

3. Morphological Effects in the Global (X-ray to radio) Emission Properties of Spiral Galaxies

It is not surprising that galaxies of different morphological types may emit differently at different wavelengths, either because of their stellar population mix, dust content, active star formation, properties of the ISM, or size and accretion efficiency of the nuclear black hole. What we attempt in this work is a first systematic look at the multi-wavelength global emission properties of spirals. While our original motivation was to see how the X-ray emission fits in the whole, and how it relates to other galaxian components and properties, this work is not biased towards the X-ray properties, because of the properties of our sample (drawn from the RC2, and with comparable biases; Paper I), and our results ought to be valid for the overall panchromatic spectrum of spirals. Comparison with established results will help establish how representative our sample is. Our panchromatic approach may uncover new relations that may shed light on some aspects of the global emission of spiral galaxies.

3.1. Correlation Strengths

In Paper I, we have found that both the significance of correlations between different emission bands and their functional relationships (correlation ‘slope’) vary with galaxy morphology. Here, we will examine first the morphological dependence of the correlation ‘strengths’, we will discuss the slopes as well in the following sections of this paper.

Summarizing the results of Paper I:

- (1) **All** correlations are very tight (probability of chance correlation $P \leq 10^{-6}$) in the late (Sc-Irr)

sample.

(2) We notice two separate groups of inter-correlated variables in the early (S0/a-Sab) sample: $L_{12\mu m}$, L_{FIR} , L_{6cm} (all with $P \leq 10^{-6}$); and L_X , L_B , L_H . In the latter group L_B is strongly correlated with both L_H and L_X ($P \leq 10^{-6}$), while no significant correlation is found between L_X and L_H . Correlations between pairs of variables belonging to different groups are weaker or absent.

(3) The results for the intermediate sample (Sb-Sbc) are somewhat intermediate: strong correlations persist among $L_{12\mu m}$, L_{FIR} , L_{6cm} and between L_B and L_H , but significant links of L_X with $L_{12\mu m}$, L_{FIR} , L_{6cm} now appear.

These results demonstrate the existence of morphological dependencies in the global emission properties of spiral galaxies, and confirm the earlier reports of such effects (FT, FGT). In late-type spirals and irregulars, the generally good correlations point to a general connection of all emission bands with the stellar component. In early-type bulge-dominant galaxies instead, the different correlations strengths observed between the two groups of three variables (X-ray, B, H) and (12 μ m, FIR, 6cm) suggest possibly unrelated emission mechanisms.

3.2. Color Effects

A closer look at the luminosity scatter diagrams (see Paper I for a full compilation) reveals that also the relative amount of emission (i.e., color) in the two bands under examination may be morphology dependent. This effect is evidenced by the comparison of best-fit bisectors for early and late samples, which are shown in two representative instances in fig. 1.

To quantify this effect for any given pair of variables, we have used the following approach: 1) Using the best-fit regression bisector of the late-type (T=5-10) sample as a reference, we have built the distributions of vertical residuals about this line, for both the T=0-2 and the T=5-10 sample. 2) We have then compared these distributions, to see if we would detect a systematic difference in their means, which would be symptomatic of a morphological dependence of the flux ratios. 3) In order to gauge the significance of these differences, we have performed two-sample tests on the two samples of residuals to derive the probability that the two distributions are both drawn from the same parent population. ASURV provides four different two-sample tests to use for censored data, which differ in the way the censored data are weighted in calculating the test statistic. These methods are Gehan’s Generalized Wilcoxon Test, the Logrank test, Peto and Peto’s Generalized Wilcoxon, and Peto and Prentice’s Generalized Wilcoxon test. We have applied all these tests in each case. Fig. 2 shows representative histograms of residuals and Table 1 tabulates the results for all the distributions of residuals which could be tested, i. e. excluding correlations with double censoring. A positive mean residual for the T=0-2 sample indicates that there is a relative excess in the Y-axis/X-axis ratio for this sample, when compared with the T=5-10 sample.

We see the well-known effect that early-type spirals tend to have redder colors (larger H/B flux ratios) than later-type spirals, reflecting their older stellar population (e.g., Aaronson, Huchra & Mould 1979). We find a similar H/X effect, while the ratio of X-ray and B fluxes is not morphology dependent. This effect may suggest a closer link of the X-ray with the B-band emission (rather than with the H-band emission), in agreement with previous reports (FT, FTG; see Paper I). The morphological dependencies of the FIR, 6cm, and $12\mu\text{m}$ scatter diagrams cannot be tested formally, because of double censoring. However, an inspection of the scatter diagrams in Paper I does not reveal any obvious offsets in the early-type versus late-type correlations, although in some cases the correlations follow different power-law relations. Relative to H, we find that early-type (bulge) galaxies tend to be underluminous in FIR, $12\mu\text{m}$ and 6cm. A similar effect is seen when we compare FIR and 6cm with B, while the B/ $12\mu\text{m}$ ratio does not appear to be morphology dependent. Comparisons with the X-rays cannot be formally tested because of double censoring. However visual inspection of the data suggests a similar behavior as that observed with B.

The relative lack of radio and far-IR emission relative to stellar and X-ray emission we observe in early-type spirals (S0/a-Sab), strengthens the possibility of unrelated emission mechanisms for these two wavebands.

3.3. Fundamental and Secondary Correlations

Comparison between different correlations can be pushed further by using conditional probability analysis (e.g. Spearman Partial Rank tests). These tests (see also Paper I) help in distinguishing between ‘fundamental’ and ‘secondary’ correlations, by giving the probability of a correlation existing between two given variables, when other variables are held fixed. Fig. 3 shows results of these tests applied to all three morphological subsamples and suggests some interesting trends. For these tests we have used all the available points for each subset of three variables under consideration, thus maximizing the significance of the results for a given test. In Paper I instead emphasis was given to the uniform analysis of the same sample observed in all six wavebands from radio to X-rays, resulting in smaller working samples.

Summarizing the results displayed in fig. 3:

- (1) There are no significant morphological dependencies in the relations among X-ray, B, and H luminosities. The only fundamental link among these variables is the strong link between B and H (see Paper I), which is present regardless of morphological type.
- (2) As reported in Paper I, we find a surprising morphological trend in the relations between $12\mu\text{m}$, FIR and 6cm luminosities, that persists in a 3-way comparison, and is strengthened by the present use of a larger sample: (a) While the FIR is always strongly correlated with the $12\mu\text{m}$ emission, the connection between IR and radio continuum is morphology dependent. (b) There is a strong fundamental link between $12\mu\text{m}$ and 6cm emission in S0/a-Sab galaxies. (c) In Sc-Irr galaxies

instead the strong link of the 6cm emission is with the FIR; note that this 3-way analysis results in a weaker and likely spurious anticorrelation between 6cm and $12\mu\text{m}$. (d) In the intermediate sample (Sb-Sbc), the result is transitional. The radio – IR link is weaker ($P \sim 1 - 2\%$) and it appears with both the $12\mu\text{m}$ and the FIR.

(3) The multivariate analysis confirms the morphology-dependent grouping of the luminosity variables in two groups, disconnected in the S0/a-Sab sample but not in the late Sc-Irr sample (see §3.1. above): (X-ray, B, H) and ($12\mu\text{m}$, FIR, 6cm). All the many-variable Spearman Partial Rank tests tabulated in Paper I suggest no connections among these two groups in early-type galaxies, while a significant link of the X-ray emission with the FIR emerges in most of the late-sample tests. Three-variable tests including the FIR, X-ray and either B or H show this effect clearly. The X-ray, H, FIR results are displayed in fig. 3.

In §4, §5 and §6 we take a closer look at these relations and discuss further their astrophysical implications.

4. The $12\mu\text{m}$ and FIR correlations

The results of the Partial Rank analysis tabulated in Paper I show that the FIR – $12\mu\text{m}$ correlation is one of the two strongest fundamental correlations (the other being H – B), regardless of morphological type and of the number of variables considered in the analysis (see also fig. 3). We find that the regression bisector slope of this correlation (α , where $L_{FIR} \propto L_{12\mu\text{m}}^\alpha$) flattens from early to late-type spirals (Paper I): 1.23 ± 0.12 in S0/a-Sab, 0.98 ± 0.07 in Sb-Sbc (T=3-4), and 0.74 ± 0.03 in Sc-Irr (T=5-10). The slopes of the early and intermediate samples are consistent with unity (a linear, everything increases at the same rate, correlation) within the errors. However, the slope of the late sample is significantly smaller than 1. Fig. 4 shows the scatter diagram for the late sample, with the regression bisector (solid line), and compares it with the bisector for the early sample (dashed line). The morphological dependency of the bisector slopes may be at least in part a luminosity effect. In particular, the T=0-2 and T=3-4 galaxies (which, within the errors, have consistent slopes) tend to be of high luminosity, while T=5-10 galaxies include a significant number of low-luminosity systems. Omitting the T=5-10 galaxies with $\text{Log}(L_{FIR} < 42.5)$, the regression slope steepens becoming close to unity. This result suggests that there may be intrinsic differences between the production of FIR and $12\mu\text{m}$ in low- and high-luminosity late-type galaxies.

We have investigated further the $12\mu\text{m}$ – FIR link by generating $12/100$ vs. $B/100$ color-color plots for the three subsamples (fig. 5). In the T=3-4 sample, the distribution of points is essentially horizontal, consistent with a constant $12/100$ ratio. This is what one would expect if the $100\mu\text{m}$ and $12\mu\text{m}$ emission both arise from the ISM in spiral galaxies (e.g. Helou, Ryter & Soifer 1991), with the $12\mu\text{m}$ emission resulting from the non-equilibrium heating of small size dust grains by the same UV photons that heat larger grains to give rise to the $100\mu\text{m}$ flux. As suggested by

Helou, Ryter & Soifer 1991 the spread in the 12/100 ratios may result from differences in the dust grain-size distribution of the ISM in different galaxies, which may in part be linked to their star-formation activity. Smaller grains would be destroyed by the more intense UV photon field of more active star-forming galaxies. In agreement with a constant 12/100 color, the 12 μ m and FIR luminosities are linearly correlated in this sample. The analogous plot for T=5-10 galaxies shows a similar distribution except for a group of galaxies which appear to be both bluer (excess of B relative to 100 μ m) and brighter in the 100 μ m band relative to the 12 μ m than the bulk of the distribution (numbered 1-7 in fig. 5). These objects belong to the group of low luminosity galaxies responsible for the flattening of the FIR – 12 μ m correlation (fig. 4). These blue dwarf galaxies may be undergoing active star formation, resulting in a depletion of small size interstellar grains. Their blue colors suggests particularly intense UV emission.

The 12/100 vs. B/100 plot for T=0-2 (S0/a-Sab) galaxies differs from those of later types in interesting ways. It presents larger scatter, with a number of points having larger 12/100 and/or B/100 ratios than in later-type galaxies. Some of these points are within the locus of E and S0 galaxies (from EFK, solid polygon in fig. 5) which are distributed mostly within a diagonal strip in this plane. This distribution suggests that the 12 μ m emission in at least some S0/a-Sab galaxies is due to photospheric and circumstellar emission of red giants [as in E and S0s, (Knapp et al. 1992), where a strong correlation between 12 μ m and B emission is observed (EFK)]. The points with Log (12/100)<0 to the left of the E and S0 swath could be explained with extinction; however, their colors are also consistent with those of later-type spirals, and may be indicative of interstellar emission. There are also points in the 12/100 vs. B/100 plot of S0/a-Sab galaxies which lie in a region outside of the observed loci of either later type spirals or E and S0s. Some of these galaxies are well known Seyferts (which were excluded from our correlation analysis; they are identified in fig. 4 by circled symbols), suggesting that this region is occupied by luminous active nuclei. There may be a cross-over of nuclear versus global galaxian emission properties, depending on the relative luminosities of these components: notice that galaxies with mini-AGNs (identified by enclosing squares, from Ho, Filippenko & Sargent 1997) tend to be in the E and S0 locus, and follow the general distribution of T=3-4 galaxies as well. Note that the strong FIR-12 μ m correlations of S0/a-Sab galaxies would exist no matter what the energy source that gets re-radiated (stars or AGN).

In summary, the results presented here show an overall connection between mid and far-IR emission in spiral galaxies, regardless of morphological type, in agreement with earlier conclusions on the interstellar origin for both IR emission bands (Helou, Ryter & Soifer 1991). However, there are complications to this picture. Discrepancies arise in bulge-dominated galaxies, where both red-giants and luminous AGN emission may play a dominant role in the 12 μ m emission of some galaxies; and in blue late-type dwarf galaxies, where star formation may be particularly active, resulting in the depletion of small size grains and relative lack of 12 μ m emission.

5. The Infrared-6cm Connection: Star Formation and Nuclear Activity

It is well known that radio continuum at 20cm and the far-infrared are correlated. This correlation, discovered soon after IRAS became operational (Dickey & Salpeter 1984; Helou, Soifer & Rowan-Robinson 1985; de Jong et al. 1985), suggests a strong connection between non-thermal radio continuum emission in galaxies and the star-forming stellar component. Its discovery resolved the debate on the origin of the radio continuum emission of spirals (Lequeux 1971; Biermann & Fricke 1977; Hummel 1990), by linking the production of relativistic electrons to SNII in the young stellar population.

As shown by our analysis (Paper I) the radio-continuum far-infrared correlation is also highly significant at 6cm, both in early- and in late-type spirals. However, when we explore the relative strengths of the correlations among 6cm, $12\mu\text{m}$, and FIR, we find intriguing significant morphological differences (§3, fig. 3) between early- and late-type spirals: in S0/a-Sab galaxies the 6cm radio continuum is directly correlated with the $12\mu\text{m}$ rather than with the FIR; in Sc and later types (T=5-10) instead the 6cm radio continuum is directly correlated with the FIR emission. These differences in the radio-continuum – IR correlations suggest different origins for the radio continuum emission of S0/a-Sab galaxies and later type spirals.

Although the 6cm emission of late-type spirals differs from the non-thermal 20cm emission, by including a fraction of thermal emission from HII regions (Gioia, Gregorini & Klein 1982), the strong FIR – 6cm link in these galaxies and the linearity of this correlation ($L_{\text{FIR}} \propto L_6^{0.91 \pm 0.06}$), are in agreement with the overall connection of radio emission and star formation, derived from 20cm measurements.

The fundamental 6cm – $12\mu\text{m}$ correlation of S0/a-Sab galaxies instead argues for a different origin of the 6cm radio continuum in these systems. This correlation appears steeper (slope = 1.79 ± 0.21) than the analogous one for the Sc-Irr sample, which has a nearly linear slope of 0.88 ± 0.07 (fig. 6), that agrees with the overall star formation picture. We suggest that nuclear activity may be responsible for the steep fundamental correlation of S0/a-Sab galaxies. As discussed in § 4, the 12/100 - B/100 color-color plot of S0/a-Sab galaxies suggests that nuclear activity may be important for their $12\mu\text{m}$ emission. Moreover, we find a remarkable similarity when we compare the 6cm – $12\mu\text{m}$ scatter plots of ‘normal’ S0/a-Sab’s and bright AGNs (fig 6a). S0/a-Sab galaxies containing bright AGNs were not included in the regression analysis (Paper I) but are plotted as circled points in the scatter diagram. Their distribution is consistent with that of the other points in the diagram, suggesting that the $12\mu\text{m}$ and 6cm emission of all these galaxies may be connected with nuclear activity. If we calculate the regression bisector, including the AGN, we find a very consistent result (slope 1.69 ± 0.17). Note that a large number of the early sample galaxies host a low-luminosity AGN (see fig. 6a).

The connection of radio-continuum emission with the mid-IR, rather than with the FIR is in itself suggestive of some kind of nuclear activity. Seyfert galaxies and QSOs tend to have significant mid-IR emission (Elvis et al. 1994). In these bright AGNs the mid-IR emission may

be due to thermal emission of circumnuclear dust heated by the intense nuclear UV continuum. Nonthermal radio and $10\mu\text{m}$ sources have also been found in the nuclei of spirals galaxies, with remarkable spatial similarities (Ho et al. 1989). In the latter type of nuclei shocks from supernovae may collisionally heat small dust grains in the nuclear region to $12\mu\text{m}$ temperatures, as well as accelerating electrons which interact with the interstellar magnetic field to produce synchrotron radiation (Ho et al. 1989). Shocks would also be effective in enriching the ISM with small-size grains, resulting in enhanced mid-IR emission. A similar picture may hold for shocks connected with supersonic outflows from an active nucleus.

While the possibility of nuclear activity as an explanation of the radio – mid-IR correlation in S0/a-Sab galaxies is attractive, the steep power-law of this correlation cannot be easily explained in either of the above two scenarios. If the correlation were due to shocks resulting from phenomena linked to star-formation, as in the Ho et al. 1989 scenario, we would expect to see more of a proportionality between radio continuum and mid-IR emission, as observed in late-type spirals. Ho et al. 1989 report such proportionality in point-to-point comparisons of their $10\mu\text{m}$ and radio continuum maps. In the alternative AGN scenario, where re-radiation of the UV continuum could be responsible for the mid-IR emission, the steep $6\text{cm} - 12\mu\text{m}$ power law could be understood if there were a similar steep dependency between the nuclear radio continuum and the higher energy nuclear continuum. If we take the X-ray emission as an indicator of the latter, and we assume that the UV continuum behaves accordingly, we should then expect to find a similar steep radio – X-ray correlation. Except for a report by Unger et al. 1987, which however includes comparison of an X-ray selected sample of active galaxies (the ‘Piccinotti’ sample; Piccinotti et al. 1982) with more powerful, optically/radio selected AGN, there is no evidence of such a trend. Within the Piccinotti sample, the radio – X-ray luminosity correlation appears linear (Unger et al. 1987). The same is true for a correlation between radio core power and X-ray luminosity in powerful 3CR galaxies (Fabbiano et al. 1984).

The above arguments suggest that if nuclear activity is responsible for the $6\text{cm} - 12\mu\text{m}$ correlation of S0/a-Sab galaxies, these nuclei do not behave either like those of more powerful AGN, or like nuclear regions where the activity may be connected with particularly intense star formation (as in Ho et al. 1989). However, a similarly steep correlation can be seen in relatively radio-quiet E and S0 (EFK), where nuclear activity (either non-thermal, e.g. Fabbiano, Gioia & Trinchieri 1989, EFK, Ho 1999, or possibly connected with nuclear star formation, e.g. Wrobel & Heeschen 1991) has also been raised as a possible explanation of the radio continuum emission. If X-ray emitting hot halos are present (see § 7) in the more luminous/massive S0/a-Sab galaxies, these halos may be responsible for diminishing their small-size dust grain population (e.g. see Dwek & Arendt 1992), resulting in a relatively less intense mid-IR emission at the higher luminosities.

We cannot exclude the possibility that S0/a galaxies alone may be responsible for the steep correlation because the slope flattens to 1.08 ± 0.12 if $T=0$ (S0/a) galaxies are excluded. However, this flattening may be due to the more restricted radio continuum luminosity range covered by

the T=1-2 galaxies in our sample (crosses in fig. 6a). In the region of overlap, S0/a's cannot be distinguished from Sa-Sab's, suggesting no major intrinsic difference. We do not find any substantial difference in the results of the multivariate partial rank analysis if we exclude the S0/a galaxies. The 6cm-12 μ m correlation is still the fundamental one. However, the sample size is in this case reduced to only 14 galaxies. Further analysis of possible morphological differences within early-type spirals will require assembling a substantially larger sample.

6. The X-ray – Star-Formation Link in Late-Type Spirals

The connection between X-ray emission and star-formation activity was first suggested by Fabbiano et al. 1982, who reported higher X/B flux ratios in bluer galaxies with disturbed morphologies, possibly resulting from a large number of luminous young massive X-ray binaries, young SNR, and some hot ISM as well (e.g. Fabbiano 1996). More recently, detailed multi-frequency high resolution images are revealing one-to-one associations between bright X-ray emitting regions and star-forming regions (e.g. in NGC4038/9, Fabbiano et al. 1997, Fabbiano, Zezas & Murray 2001). FGT (see also Fabbiano 1990) first discussed the X-ray – FIR correlation in spiral galaxies and connected it with the star-forming galaxian component. Subsequently, David et al. 1992 reported a connection between X-ray emission and FIR in the IRAS Bright Galaxy Sample. This sample, however, includes early, intermediate, and late-type spirals, which, as we have now shown, differ in their integrated emission properties.

As discussed in Paper I, the results of the multivariate – X-ray, B, H, 12 μ m, FIR, 6cm – conditional probability analysis point to the central role of star-formation in the global emission properties of Sc-Irr galaxies. In these galaxies there are strong intrinsic correlations of mid-IR and radio continuum with the FIR (Paper I). A possible, although weaker, link of X-ray and FIR is also revealed in most of the tests in Paper I (see fig. 3). Added support is provided by the existence of a significant correlation of the L_X/L_B luminosity ratio in late-type spiral galaxies with the L_{60}/L_{100} ratio (Paper I). The latter is a measure of the FIR color-temperature. Warm FIR color-temperatures (higher L_{60}/L_{100} ratios) have been associated with star-formation activity (e.g., Helou, Rytter & Soifer 1991). They have been found to occur *both* in high luminosity spirals, suggesting the presence of hidden star forming regions in large disk galaxies, and in blue H α -bright galaxies, where the association with star formation is more immediate (Trinchieri, Fabbiano & Bandiera, 1989 (TFB) and refs. therein). Therefore, the correlation of the L_X/L_B excess with L_{60}/L_{100} reinforces the link between L_X/L_B and star-formation.

Table 2 summarizes the regression bisectors for the late sample (from Paper I) and also gives bisectors obtained by omitting from the sample the seven blue/FIR-bright dwarfs which appear a group apart in fig. 5. The correlations between X-ray, FIR and 6cm luminosities all follow power-law slopes near 1, consistent with a related origin through star formation, and with the fact that these three emission bands are relatively little affected by extinction – the X-rays are some, but much less than the optical band. However, in the restricted higher luminosity sample

the X-ray - 6cm correlation departs significantly from linearity. This flatter slope results from the omission of a single low-luminosity detection from the sample and as such the result calls for future confirmation. If confirmed, it would be consistent with the X-ray – radio-continuum slope found by FGT.

Based on a Partial Rank analysis of a small sample of 17 T= 4 – 10 galaxies, FGT suggested a direct link between X-ray and radio continuum emission in late-type spirals. Our present analysis does not confirm this suggestion. If we analyse the correlations among X-ray, FIR and 6cm, with the 53 T= 5 – 10 galaxies for which fluxes are available in all these three variables, we find that two correlations are significant, X – FIR ($P = 0.007$) and FIR – 6cm ($P < 0.005$), the latter being by far the most significant. There is no direct statistical link between X and 6cm. Thus we conclude that the X-ray – radio continuum correlation is likely to arise from the connection of both emission bands with star-formation in disk/arm dominated galaxies, rather to indicate a direct physical link between X-ray and cosmic ray sources.

7. The Steep X-ray – B Correlation

The $L_X - L_B$ correlation has been the subject of much attention in X-ray studies of normal galaxies of all morphological types (e.g. Fabbiano 1989, EFK), and it has been used to gain understanding on the nature and origin of the X-ray emission. However, our larger sample shows that this correlation is not a fundamental one in spiral galaxies (Paper I). In early-type spirals there is no strong fundamental link between X-rays and any of the other emission bands. In late-type spirals there is a significant - but not overly strong - link only with the FIR (Paper I; § 3; § 6). Perhaps, all the emphasis put into the study of this correlation is unwarranted. However, even if this correlation is not the result of a direct causal link, we can still learn by looking at it more closely.

We find (Paper I) that the $L_X - L_B$ relationship is significantly steeper than linear in spirals, with slopes of 1.45 ± 0.15 in S0/a-Sab galaxies, 1.53 ± 0.17 in Sb-Sbc, and 1.48 ± 0.13 in Sbc-Irr. These results differ from previous reports of a linear (power-law slope 1) relation between the X-ray and B-band luminosities of spiral galaxies (FT; FGT), which suggested a link between the bulk of the X-ray emission and populations of evolved stellar sources (e.g. X-ray binaries, SNRs; see Fabbiano 1989), belonging to the same stellar component responsible for the blue light. However, the earlier work was based on a much smaller sample of galaxies than presently available (51 versus 234). While all these power-law slopes are statistically consistent with each other, there are considerations that support an intrinsic difference in the phenomena responsible for the bulk of the X-ray emission in early- and late-type spirals. We have discussed in § 6 the linear X-ray – FIR correlation of the late sample, which suggests that the non-linear X-ray – B correlation of late-type spirals and irregulars may arise from extinction in star-forming complexes in the most luminous galaxies. Extinction would affect the B band more than the X-rays, causing a deviation from linearity (§ 8). This explanation does not apply easily to early-type spirals, where dusty

active star-forming regions are rare.

The nature of the X-ray emission of early-type, prominent-bulge spirals has been the subject of an on-going controversy, which has sought to establish if and how much of this emission can be ascribed to the thermal emission of an optically thin hot gaseous medium, that may be used to measure the mass of the parent galaxy (Forman, Jones & Tucker 1985, FT, Trinchieri & Fabbiano 1985, FGT, Kim, Fabbiano & Trinchieri 1992, Fabbiano & Juda 1997, Terashima et al. 1994), in addition to the X-ray binary population that must be present (e.g. Fabbiano 1989) and it is now seen directly in Chandra images (e.g. Irwin, Bregman & Sarazin 2000). Detailed hydrodynamical models developed for S0 galaxies may apply, and suggest that although large static halos are not expected, hot ISM in a complex flow state may be found (D’Ercole & Ciotti 1998). The steep X-ray – B correlation may suggest the presence of gaseous halos in X-ray luminous S0/a-Sab galaxies, by analogy with the similarly steep correlation observed in E and S0 galaxies (Trinchieri & Fabbiano 1985, Canizares, Fabbiano & Trinchieri 1987, EFK, see also the ASCA results of Matsumoto et al. 1997). Supporting evidence is provided by X-ray spectral data. The average *Einstein* X-ray colors of Sa galaxies are similar to the colors of S0 and E galaxies where hot halos are found, rather than to those of later types, which are characterized by harder X-ray spectra, typical of X-ray binaries (Kim, Fabbiano & Trinchieri 1992). ASCA higher resolution CCD spectra of NGC 4594 (Terashima et al. 1994) and NGC 4736 (Roberts, Warwick & Ohashi 1999) also support the presence of a thermal gaseous component in these galaxies, which is confirmed in NGC 4736 by the high spatial/spectral resolution Chandra ACIS-S image (Pellegrini et al. 2001; another recent example of a Chandra observation that shows both a population of point-like sources and diffuse emission is the S0/a NGC 1291 Irwin, Bregman & Sarazin 2000).

‘Hidden’ AGNs may in principle add to the X-ray emission and cause a steep X-ray – correlation. However, we believe that this is unlikely. Fig. 7 shows that luminous AGNs indeed have very significant X-ray excess luminosity, but their distribution is not consistent with the high luminosity extrapolation of the X-ray – B correlation. A large number of galaxies in this sample host mini-AGNs (Ho, Filippenko & Sargent 1997, see fig 7), but it is unlikely that the X-ray luminosity of these galaxies is dominated by this emission. This conclusion is supported by X-ray imaging for at least two X-ray luminous galaxies: NGC 4594 (Fabbiano & Juda 1997, Ho et al. 2001; a LINER galaxy with a compact nuclear radio source, Heckman 1980, Condon et al. 1982) and NGC 4736 (M94; Cui et al. 1997, Roberts, Warwick & Ohashi 1999, Pellegrini et al. 2001); in both galaxies the nucleus does not dominate the emission in the soft X-ray band. In NGC 4736, in particular, the Chandra image shows that the nucleus is not even the most luminous source in the central region of this galaxy (Pellegrini et al. 2001). Moreover, a recent high resolution Chandra survey of a number of mini-AGN galaxies shows in the majority of them nuclear sources with luminosities well below the total galaxian emission (Ho et al. 2001).

8. Non-Linear Power-Law Dependencies in Disk/Arm-Dominated Spirals: extinction and other effects

We have mentioned earlier in this paper and shown in Paper I that in the late (T=5-10; Sc-Irr) sample all the correlations are highly significant. We have also discussed how some of these correlations (e.g. X-ray – FIR) are close to a power-law of slope 1. Others (e.g. B – H, X-ray – B) are not (Table 2).

Extinction in dusty star-forming regions may be responsible for some of these departures from linearity. Extinction would affect the B emission more than longer wavelengths such as H, $12\mu\text{m}$, FIR, 6cm, or higher energies such as the X-rays. The $L_B \propto L_{FIR}^{0.7}$ relation was first observed by FGT, and explained (see also TFB) with an enhanced dusty compact starburst component in higher-luminosity galaxies. This scenario would also account for the flat $L_B - L_{6cm}$ power-law: the longer wavelength radio-emission from the star-burst component would not be obscured by the dust in these star-forming regions, and so would scale linearly with the FIR and according to the observed power-law with the optical. The X-ray – B relationship is also not linear, and it could be consistent with the obscuration picture. Assuming 2.5 magnitudes of visual extinction, which is the average value required to explain the departure from linearity of the FIR – B correlation (FGT), we find that the corresponding extinction in the X-ray emission would only be $A_X \leq 0.5$ mag, much less than the extinction in B. Although $A_V = 2.5$ mag exceeds the average galaxian extinction, a large amount of obscuration is present in localized star-forming regions (e.g. Engelbracht et al. 1996). A comparison of X-ray and other waveband emissions in the Antennae galaxy (NGC 4038/9; Fabbiano et al. 1997) supports the above picture. Intense X-ray, radio, and IR emission regions are co-spatial with the HII regions and nuclear region of this merger galaxy. Considering that the H-band emission is significantly enhanced by red supergiants in dusty star-forming regions (e.g. Engelbracht et al. 1996), the same star-formation/extinction scenario may naturally explain the flat power-law $L_B \propto L_H^{0.7}$, discovered by Aaronson, Huchra & Mould 1979.

The FIR – $12\mu\text{m}$ departure from linearity has been discussed in §4 and ascribed at least in part to the effect of low-luminosity blue galaxies with large FIR/ $12\mu\text{m}$ ratios. However, Table 2 shows that after these galaxies are removed the correlation is still flatter than linear. This flat FIR- $12\mu\text{m}$ correlation may be responsible for the flatter relations of B (and X-rays) with $12\mu\text{m}$ than with FIR. A possible explanation for this residual effect – to be checked with future IR data – is that our sample is still contaminated by some ‘blue dwarf’ galaxies at the low-luminosity end.

9. Summary and Conclusions

We have performed (Paper I) a statistical analysis of 234 normal spiral galaxies from the sample of FKT, which were all observed in X-rays with the *Einstein Observatory*. This analysis explores relations among 6 emission bands, including X-rays (0.2-4 keV), B, H, $12\mu\text{m}$, FIR, and

6cm, in the entire sample of 234 galaxies and in subsamples comprising S0/a-Sab, Sb-Sbc, and Sc-Irr galaxies respectively. In this paper we report morphology-related effects in these results. We also explore the implications of our results for the emission processes of early- (S0/a-Sab) and late-type (Sc-Irr) galaxies separately. The main conclusions of this paper are summarized below:

(1) Bivariate and multivariate correlation analyses suggest clear morphological dependencies of the global radio-IR-optical-X-ray emission properties:

- in late-type galaxies (Sc-Irr), all the emission properties are correlated suggesting a broad connection to the galaxian stellar population;
- in early-type spirals (S0/a-Sab) instead, $12\mu\text{m}$, FIR, and 6cm emissions are not connected with either the stellar population responsible for the global near-IR and optical light (H and B) or with the X-ray emission.
- the intermediate sample of Sb-Sbc (T=3-4) galaxies presents intermediate properties, with some links appearing between X-rays and FIR.

(2) The strong, always present, fundamental $12\mu\text{m}$ and FIR correlation (see also Paper I) agrees with the picture that both emission bands are due to the same photon field interacting with different size grains (Helou, Rytter & Soifer 1991). However, we also find some effects that point to morphology-related differences in the IR emission processes, and possibly to different (stellar and AGN) sources of radiation in different types of galaxies:

- The 12/100 vs. B/100 color-color plot of S0/a-Sab galaxies presents more scatter than those of later morphological types, that could be explained with both significant red giant circumstellar dust (as in ellipticals and S0s, Knapp et al. 1992), and nuclear emission.
- Blue late-type dwarf galaxies appear to be underluminous in the mid-IR, suggesting that the composition of the ISM in these galaxies lacks the small grains responsible for the mid-IR emission. This difference may be related to the more intense UV field, suggested by their blue colors.

(3) Our results suggest a difference in the production of radio continuum and IR emission in early- and late-type spirals.

- In Sc-Irr galaxies we find a fundamental, strong, linear radio – FIR correlation, consistent with the previously reported connection of the radio continuum emission with the star-forming stellar population (e.g., Helou, Soifer & Rowan-Robinson 1985).
- In S0/a-Sab galaxies instead the fundamental radio – infrared link is the 6cm – $12\mu\text{m}$ correlation, and this correlation is steeper than linear ($L_{6\text{cm}} \propto L_{12}^{1.79 \pm 0.21}$). We propose nuclear activity as the source of this correlation: the close link with the mid-IR argues in itself for this possibility, since mid-IR emission is enhanced in AGN (Elvis et al. 1994); moreover, the correlation is also consistent with the distribution of bright AGNs in the same diagram. The power-law slope of this correlation is however difficult to explain. Linear correlations would be expected both in the picture of shock-related nuclear emission (e.g., Ho et al. 1989), and in the more traditional

AGN scenario, where the IR emission may be due to re-radiation of the nuclear continuum. The observed non-linearity may be related to the presence of hot gaseous halos in the more luminous galaxies, which may result in depletion of small-size dust grains (and thus a decrease of the 12μ flux). A similar mechanism may operate in E and S0 galaxies, where a steep radio – IR correlation has also been reported (EFK).

(4) In Sc-Irr galaxies the strongest link of the X-ray emission with a stellar indicator is the linear X-ray – FIR correlation. Conditional probability analysis shows that this is a far more significant link than the X-ray – B one, suggesting a connection of the X-ray emission with the star forming stellar component. This conclusion is reinforced by the $L_X/L_B - L_{60}/L_{100}$ correlation found in Paper I, which associates more intense X-ray emission with hotter IR colors. We find no evidence of a strong intrinsic link of X-ray and radio continuum emission, contrary to the early suggestion of FGT.

(5) Contrary to previous reports, based on much smaller samples (FT, FGT), the X-ray – B correlation is steeper than linear ($L_X \sim L_B^{1.5}$), regardless of morphological type.

– In the light of the stronger linear X-ray – FIR correlation, in Sc-Irr this slope may be explained with absorption of the blue light in dusty intense X-ray emitting star-forming regions in bright galaxies.

– In S0/a-Sab galaxies it suggests the presence of an additional emission component, dominating the X-ray emission of the more luminous galaxies. Comparisons with the analogous correlation observed in E and S0s, and with the distribution of AGNs in the $L_X - L_B$ plot, suggest that hot ISM in X-ray brighter galaxies (as in E and S0s), rather than nuclear activity may be the more viable explanation.

(6) Finally, examining the power-law slopes of the correlations in the late-type spirals (T=5-10), we find linear and non-linear correlations. These different slopes may be related to the prevalence of obscured starforming regions in higher luminosity galaxies, as discussed in FGT.

Given the characteristics of our sample and the analysis techniques employed we believe these results to be free from strong biases (Paper I), and therefore to be representative of the characteristics of normal spiral galaxies. This conclusion is reinforced by the general agreement with previous IR-based work by other authors, using different representative samples of spiral galaxies. However, to confirm and expand these results, the assembly of larger, well defined, possibly complete, samples of spiral galaxies with multi-wavelength coverage is needed. Our results suggest many lines of future investigations: a re-examination of the radio continuum – IR correlations and their morphological dependencies; high resolution observations of early-type spirals in the X-rays, mid-IR, and radio continuum, to isolate nuclear sources in these bands, and to quantify the amount of hot ISM in the X-rays; comparison with optical emission line properties, to further explore the presence and properties of low-luminosity active nuclei; multi-wavelength imaging of luminous late-type galaxies to confirm the impact of dusty star-forming regions in their overall emission.

We thank Paul Eskridge and Martin Elvis for comments and Steve Willner for discussions on the near-IR emission. This work was supported by NASA grants NAG 5–2281 and NAG 5–1937 (*ROSAT*); NAGW–2681 (LTSA); and by NASA contract NAS 8–39073 (Chandra X-ray Center).

REFERENCES

- Aaronson M., Huchra, J., Mould, J. 1979, ApJ, 229, 1.
- Biermann, P. & Fricke, K. 1977, A&A, 54, 461.
- Canizares, C. R., Fabbiano, G., Trinchieri, G. 1987, ApJ, 312, 503
- Cui, W., Feldkhun, D., Braun, R. 1997, ApJ, 477, 693
- Condon, J.J., Condon, M.A., Gisler, G., Purcell, J. J. 1982, ApJ, 252, 102
- de Jong, T., Klein, U., Wielebinski, R., Wunderlich, E. 1985, A&A, 147, L6
- D’Ercole, A. & Ciotti, L. 1998, ApJ, 494, 535
- de Vaucouleurs, G., de Vaucouleurs A., Corwin, H.G. 1976, Second Reference Catalogue of Bright Galaxies (Austin: University of Texas Press)
- David, L. P., Jones, C., Forman, W. 1992, ApJ, 388, 82
- Dickey, J.M., Salpeter, E. E. 1984, AJ, 284, 461
- Dwek, E., Arendt, R.G., 1992, Ann.Rev.A.Ap., 30, 11
- Elvis, M., Wilkes, B. J., McDowell, J. C., Green, R. F., Bechtold, J., Willner, S. P., Oey, M. S., Polomski, E., Cutri, R. 1994, ApJS, 95, 1
- Engelbracht, C. W., Rieke, M.J., Rieke, G. H., Latter, W. B. 1996, Ap. J., 467, 227.
- Eskridge, P.B., Fabbiano, G., Kim, D.-W. 1995, ApJS, 97, 141 [EFK]
- Fabbiano, G. 1989, Ann.Rev.A.Ap., 27, 87.
- Fabbiano, G. 1990 in *Windows on Galaxies*, eds. G. Fabbiano, J.S. Gallagher, A. Renzini, p. 231. Dordrecht: Kluwer
- Fabbiano, G. 1996, in *Röntgenstrahlung from the Universe*, ed. H. U. Zimmermann, J. E. Truemper & H. Yorke, MPE Report 263, p. 347
- Fabbiano, G., Feigelson, E., & Zamorani, G. 1982, ApJ, 256, 397
- Fabbiano, G., and Juda, J.Z. 1997, Ap. J., 476, 666
- Fabbiano, G., Trinchieri, G. 1985, ApJ, 296, 430 (FT)
- Fabbiano, G., Trinchieri, G. 1987, ApJ, 315, 46.
- Fabbiano, G., Gioia, I.M, Trinchieri, G. 1988, ApJ, 324, 749 (FGT)

- Fabbiano, G., Gioia, I.M, Trinchieri, G. 1989, ApJ, 347, 127
- Fabbiano, G., Kim, D.-W., Trinchieri, G. 1992, ApJS, 80, 531. (FKT)
- Fabbiano, G., Miller, L., Trinchieri, G., Longair, M., Elvis, M. 1984, ApJ, 277, 115.
- Fabbiano, G., Schweizer, F., Mackie, G. 1997, ApJ, 478, 542
- Fabbiano, G., Zezas, A., & Murray, S. S. 2001, ApJ, 554, 1035
- Forman, W., Jones, C., Tucker, W. 1985, ApJ, 293, 102
- Gallagher, J, Fabbiano, G. 1990, in *Windows on Galaxies*, eds. G. Fabbiano, J.S. Gallagher, A. Renzini, p.1. Dordrecht: Kluwer
- Gioia, I.M., Gregorini, L., Klein, U. 1982, A&A, 116, 164
- Gunn, J.E., Stryker, L.L., Tinsley, B. M. 1981, ApJ, 249, 48
- Heckman, T.M. 1980, A&A, 87, 152
- Helou, G., Soifer, B.T., Rowan-Robinson, M. 1985, ApJ, 298, L7.
- Helou, G., Ryter, C., Soifer, B.T. 1991, ApJ, 376, 505.
- Ho, L. C., Filippenko, A. V., & Sargent, W. L. W. 1997, ApJS, 112, 315
- Ho, L. C. 1999, ApJ, 510, 631
- Ho, L. C. et al 2001, ApJ(letters), 549, L51
- Ho, P. T., Turner, J. L., Fazio, G., Willner, S. P. 1989, ApJ, 344, 135
- Hummel, E. 1980, Ph. D. Thesis, Univ. of Groningen, Netherlands
- Hummel, E. 1990, in *Windows on Galaxies*, eds. G. Fabbiano, J.S. Gallagher, A. Renzini, p. 141, Dordrecht: Kluwer
- Irwin, J. A., Bregman, J. N., Sarazin, C. L. 2000, AAS, 197111.14
- Isobe, T., Feigelson, E.D., Nelson, P.I. 1986, ApJ, 306, 490.
- Kendall, M., Stuart, A. 1976, *The Advanced Theory of Statistics*, Vol. 2 (New York: Macmillan)
- Kim, D.-W., Fabbiano, G., Trinchieri, G. 1992, ApJ, 393, 134
- Knapp, G.R., Gunn, J.E., Wynn-Williams, C.G. 1992, ApJ, 399, 76
- LaValley, M.P., Isobe, T., Feigelson, E.D. 1992, BAAS, 24, 839.

- Lequeux, J. 1971, *A&A*, 15, 42.
- Matsumoto, H., Koyama, K., Awaki, H., Tsuru, T., Loewenstein, M., Matsushita, K. 1997, *ApJ*, 482, 133
- Palumbo, G.G.C., Fabbiano, G., Fransson, C., Trinchieri, G. 1985, *ApJ*, 298, 259.
- Pellegrini, S. et al 2001, in preparation
- Piccinotti, G., Mushotzky, R.F., Boldt, E.A., Holt, S.S., Marshall, F.E., Serlemitsos, P.J., Shafer, R.A. 1982, *ApJ*, 253, 485
- Roberts, M.S., Hogg, D.E., Bregman, J.N., Forman, W.R., Jones, C. 1991, *ApJS*, 75, 751
- Roberts, T. P., Warwick, R. S. & Ohashi, T. 1999, *MNRAS*, 304, 52
- Shapley, A., Fabbiano, G., Eskridge, P. B. 2001, *ApJS*, in press (Paper I).
- Unger, S. W., Lawrence, A., Wilson, A. S., Elvis, M., Wright, A. E. 1987, *MNRAS*, 288, 521
- Terashima, Y., Serlemitsos, P. J., Kunieda, H., and Iwasawa, K. 1994 , in ‘New Horizon of X-Ray Astronomy - First results from ASCA’, F. Makino and T. Ohashi eds., (Tokyo: Universal Academy Press), p. 523
- Tully, B.R, Mould, J. R. & Aaronson, M. 1982, *ApJ*, 2557, 527.
- Trinchieri, G., Fabbiano, G. 1985, *ApJ*, 296, 447
- Trinchieri, G., Fabbiano, G., Bandiera, R. 1989, *ApJ*, 342, 759 (TFB).
- Young, J.S. in *Windows on Galaxies*, eds. G. Fabbiano, J.S. Gallagher, A. Renzini, p. 213, Dordrecht: Kluwer.
- Watson, M.G., Stanger, V., Griffiths, R.E. 1984, *ApJ*, 286, 144
- Wrobel, J.M., Heeschen, D.S. 1991, *AJ*, 101, 148

Fig. 1.— Scatter plots of $L_X - L_{FIR}$ and $L_H - L_{FIR}$ for the early (T=0-2, S0/a-Sab only) and late (T=5-10, Sc-Irr) samples. The solid lines represent the best-fit regression bisectors. The dashed lines on the early sample plots represent the corresponding late samples regression bisectors. Filled squares represent galaxies detected in both axes; circles represent upper limits in both axes; left-pointing triangles represent X-axis upper limits; down-pointing triangles represent Y-axis upper limits; squares surrounding other symbols are galaxies with mini-AGNs (Ho, Filippenko & Sargent 1997)

Fig. 2.— Histograms of residuals (in L_X) relative to the best-fit regression bisector of the $L_X - L_{FIR}$ correlation of the late (T=5-10, Sc-Irr) sample. Top: for the late sample. Bottom: for the early (T=0-2; S0/a-Sab) sample.

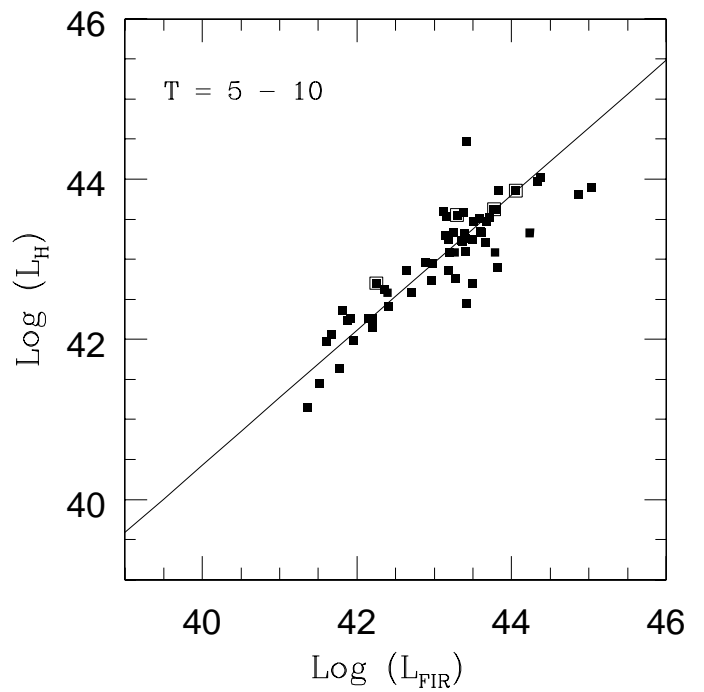
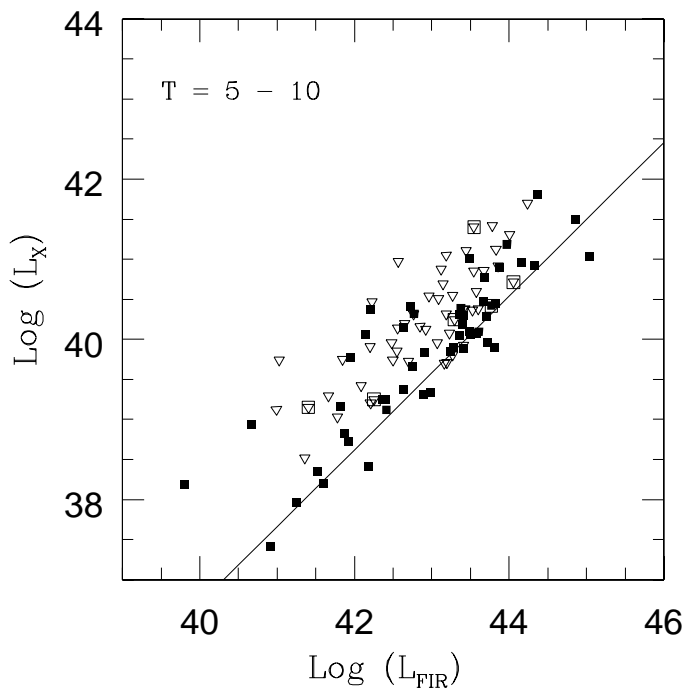
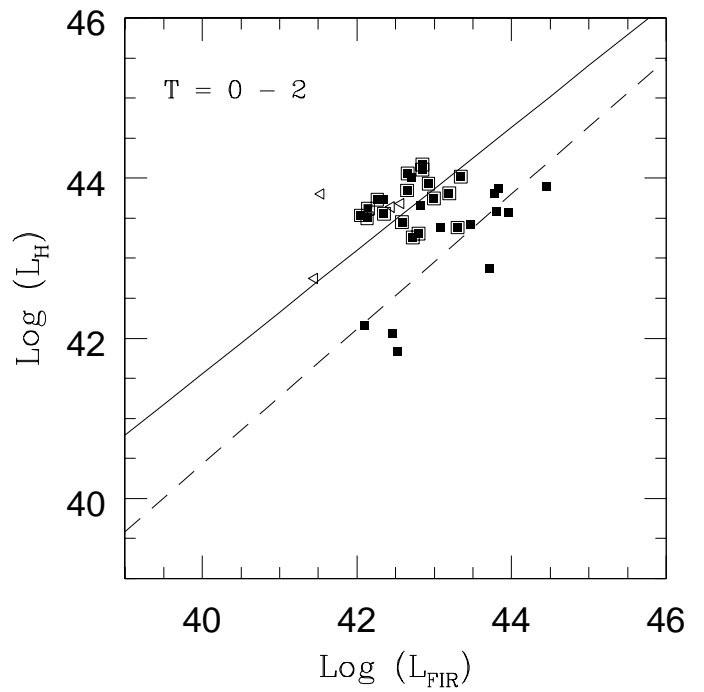
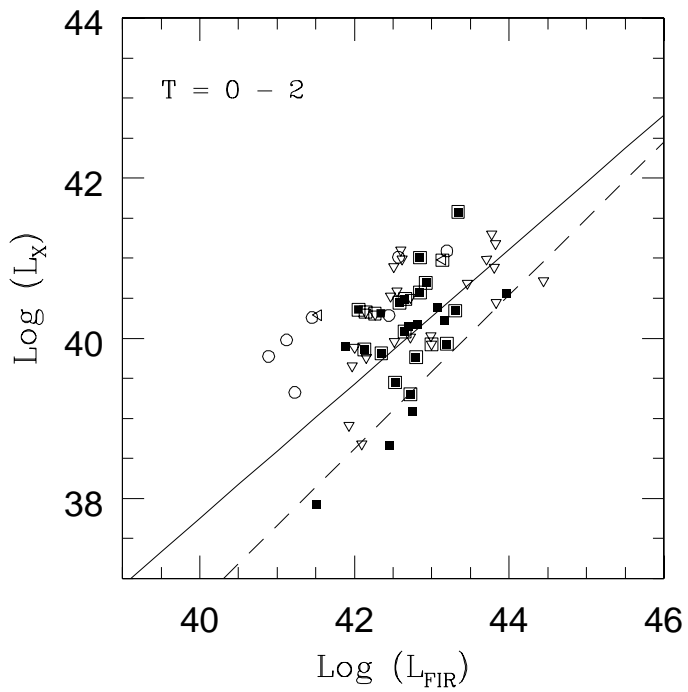
Fig. 3.— Summary of 3-variables Partial Rank results: B, H, X-ray (top), FIR, $12\mu\text{m}$, 6cm (middle), and X-ray, H, FIR) (bottom), for the three morphological subsamples. Test statistics and probabilities (see Paper I) are given for each correlation. Two connecting lines represent very significant correlations ($P < 0.005$); one connecting line represents significant correlations ($P \leq 0.03$); and no line represents a lack of significant correlation. The number of objects included in the test is given at the center of each diagram.

Fig. 4.— FIR – $12\mu\text{m}$ scatter diagram for Sc-Irr galaxies (T=5-10). Same symbols as in fig. 1, except for numbers identifying the blue dwarfs of fig. 4. The solid line is the regression bisector for the entire late-sample fit. The dotted line is the bisector of the early-sample.

Fig. 5.— $12/100$ vs. $B/100$ plot for the early (T=0-2), intermediate (T=3-4), and late (T=5-10) samples. Bright AGN points are surrounded by circles; these were not included in the correlation analysis. Triangles represent upper limits. Squares surrounding other symbols are galaxies with mini-AGNs (Ho, Filippenko & Sargent 1997). The area outlined in the T=0-2 plot identifies the region occupied by S0 (from EFK). Blue FIR-bright dwarves are labelled in the T=5-10 plot: 1=IC 1613; 2=NGC 4236; 3=NGC 247; 4=NGC 4244; 5=SMC; 6=IC 2574; 7=NGC 6822.

Fig. 6.— $L_{6cm} - L_{12}$ correlation for S0/a-Sab (a), and Sc-Irr (b) galaxies. Filled squares are detections in both variables, downward pointing triangles are upper limits in L_{6cm} , leftward pointing triangles are upper limits in L_{12} , and circles are limits in both variables. Circled points in fig. (a) represent known bright AGN, which were not included in the fit; crosses represent S0/a galaxies. Diagonal lines represent the best-fit regression bisectors. Squares surrounding other symbols are galaxies with mini-AGNs (Ho, Filippenko & Sargent 1997).

Fig. 7.— $L_X - L_B$ diagram for S0/a-Sab galaxies. Filled squares are detections, triangles are upper limits in L_X . The diagonal lines represent the best-fit regression bisectors. The circled points at the top of the S0/a-Sab scatter diagram represent known bright AGN, which were not included in the fit. Squares surrounding other symbols are galaxies with mini-AGNs (Ho, Filippenko & Sargent 1997).



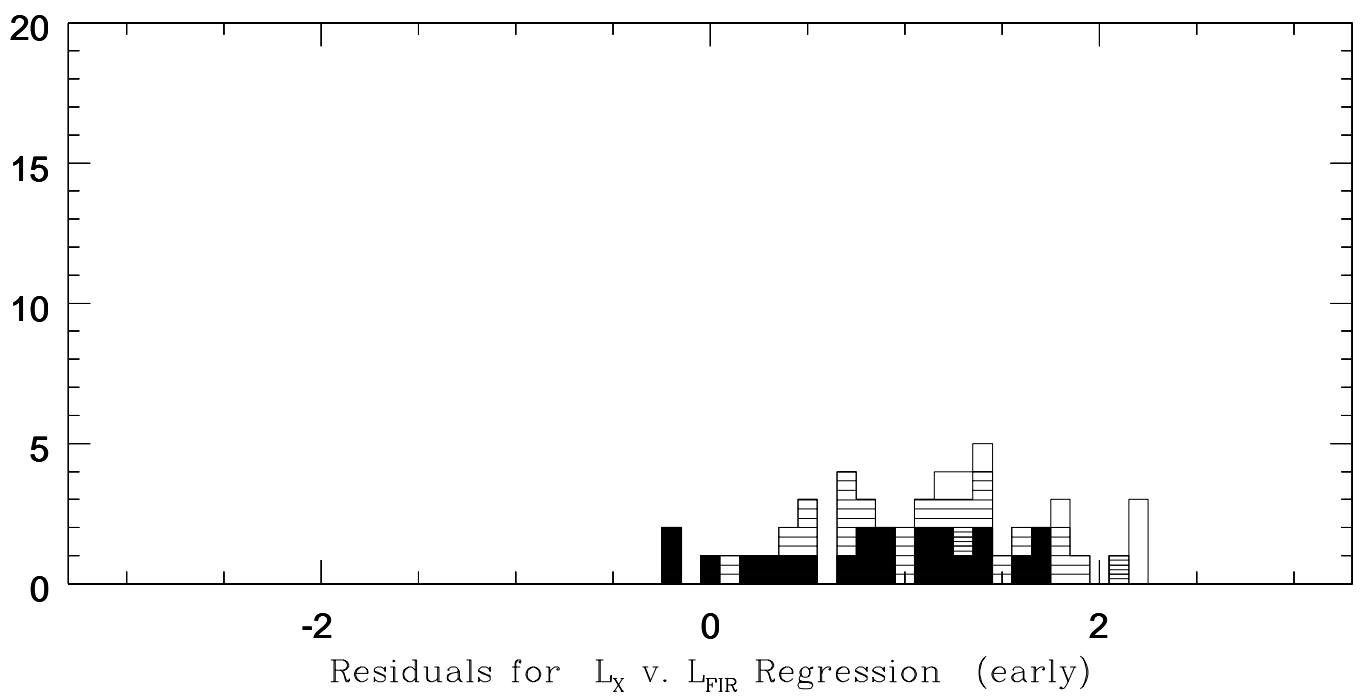
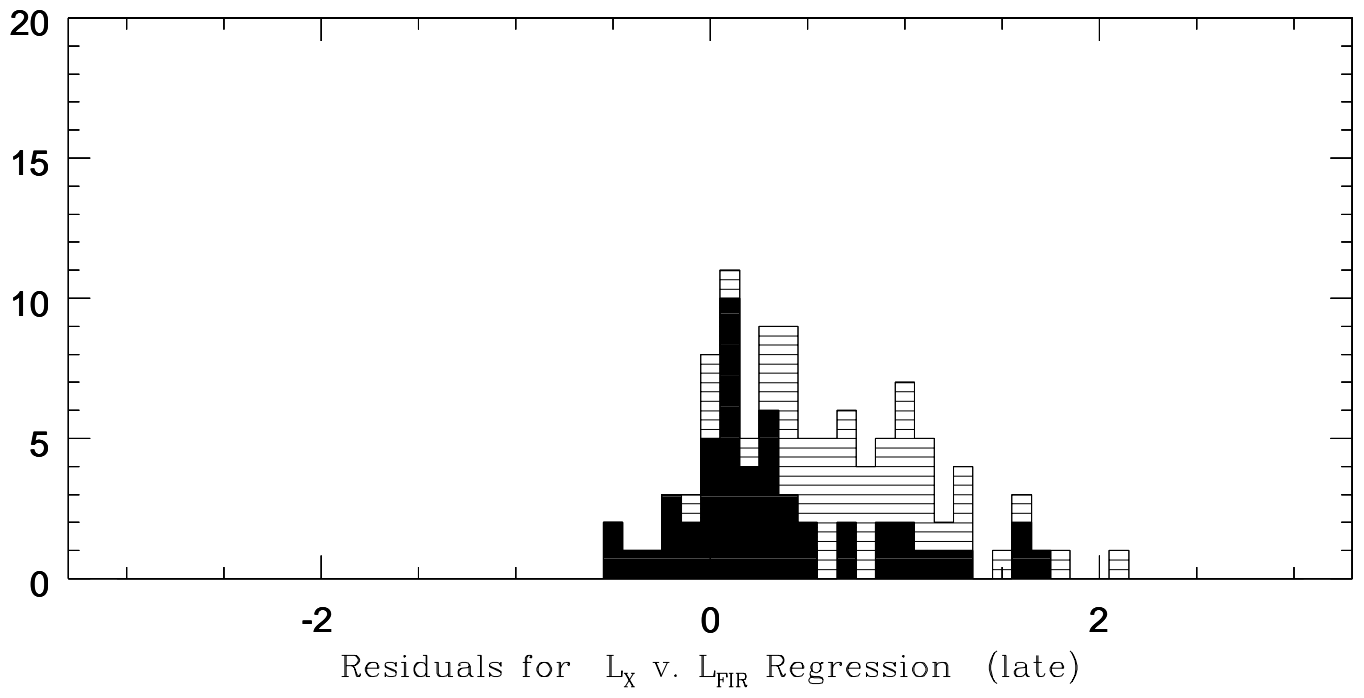


TABLE 1
RESIDUALS FOR EARLY AND LATE SAMPLES

Pair (Y, X)	Mean Residual $T = 5 - 10$	Mean Residual $T = 0 - 2$	Prob 1 ^a	Prob 2 ^b	Prob 3 ^c	Prob 4 ^d	Prob 5 ^e
B,X	-0.147 ± 0.046	-0.206 ± 0.044	0.7961	0.7932	0.2520	0.4899	0.4918
X,B	0.217 ± 0.068	0.304 ± 0.065	0.7961	0.7932	0.2520	0.4899	0.4918
B,H	0.011 ± 0.024	-0.260 ± 0.028	0.0000	0.0000	0.0000	0.0000	...
H,B	-0.016 ± 0.033	0.355 ± 0.038	0.0000	0.0000	0.0000	0.0000	...
B,12	-0.109 ± 0.035	0.009 ± 0.059	0.1108	0.1199	0.0602	0.0623	0.0623
12,B	0.243 ± 0.077	-0.018 ± 0.132	0.1108	0.1199	0.0602	0.0623	0.0623
B,FIR	0.000 ± 0.027	0.392 ± 0.068	0.0000	0.0000	0.0000	0.0000	0.0000
FIR,B	0.003 ± 0.041	-0.591 ± 0.102	0.0000	0.0000	0.0000	0.0000	0.0000
B,6cm	-0.029 ± 0.066	0.412 ± 0.103	0.0008	0.0008	0.0001	0.0004	0.0002
6cm,B	0.048 ± 0.107	-0.659 ± 0.165	0.0008	0.0008	0.0001	0.0004	0.0002
H,X	-0.044 ± 0.086	0.190 ± 0.075	0.0092	0.0114	0.0158	0.0055	0.0051
X,H	0.051 ± 0.104	-0.230 ± 0.090	0.0092	0.0114	0.0158	0.0055	0.0051
H,12	-0.001 ± 0.064	0.497 ± 0.079	0.0000	0.0000	0.0000	0.0000	0.0000
12,H	0.001 ± 0.106	-0.832 ± 0.132	0.0000	0.0000	0.0000	0.0000	0.0000
H,FIR	-0.047 ± 0.045	0.898 ± 0.108	0.0000	0.0000	0.0000	0.0000	0.0000
FIR,H	0.054 ± 0.054	-1.067 ± 0.129	0.0000	0.0000	0.0000	0.0000	0.0000
H,6cm	-0.017 ± 0.100	0.832 ± 0.160	0.0001	0.0001	0.0000	0.0001	0.0000
6cm,H	0.022 ± 0.125	-1.040 ± 0.200	0.0001	0.0001	0.0000	0.0001	0.0000

^aProbability that early- and late-type distributions of residuals are drawn from the same parent population, using Gehan's Generalized Wilcoxon Test - Permutation Variance method.

^bSame as a, but according to Gehan's Generalized Wilcoxon Test - Hypergeometric Variance method.

^cSame as a, except using Logrank Test method.

^dSame as a, except using first Peto & Peto Generalized Wilcoxon Test method.

^eSame as a, but according to Peto & Prentice Generalized Wilcoxon Test method. In the absence of censored data (as in the B,H pair), the Peto & Prentice test reduces to Gehan's Generalized Wilcoxon Test.

TABLE 2
SCHMITT’S METHOD REGRESSION BISECTORS, $T = 5 - 10$ SAMPLE

X	Y	Slope	σ_S	Int.	Blue Dwarves Removed		
					Slope ^a	σ_S^a	Int. ^a
L_B	L_X	1.48	0.13	-23.61	1.44	0.14	-21.81
L_H	L_X	1.20	0.13	-12.03	1.09	0.13	-7.05
L_{12}	L_X	0.66	0.06	12.26	0.81	0.07	5.75
L_{FIR}	L_X	0.96	0.06	-1.60	1.00	0.07	-3.42
L_{6cm}	L_X	0.90	0.07	7.70	0.79	0.06	11.81
L_H	L_B	0.73	0.04	11.34	0.74	0.05	10.87
L_{12}	L_B	0.45	0.04	23.99	0.60	0.04	17.40
L_{FIR}	L_B	0.66	0.04	14.34	0.67	0.05	13.80
L_{6cm}	L_B	0.62	0.07	20.64	0.61	0.07	21.03
L_{12}	L_H	0.60	0.05	17.89	0.75	0.07	11.45
L_H	L_{FIR}	1.19	0.09	-7.99	1.15	0.11	-6.27
L_H	L_{6cm}	1.25	0.23	-18.27	1.25	0.20	-18.27
L_{12}	L_{FIR}	0.74	0.03	11.99	0.86	0.03	6.91
L_{12}	L_{6cm}	0.88	0.07	-1.37	0.98	0.08	-5.66
L_{6cm}	L_{FIR}	0.91	0.06	10.67	0.87	0.04	12.23

^a Regression coefficients computed with blue dwarf galaxies excluded. Galaxies removed from the sample for this analysis are: NGC 6822, SMC, NGC 4236, IC 2574, NGC 4244, NGC 247, IC 1613. These blue late-type dwarf galaxies appear as a distinct population in Fig. 8, possibly indicating an ISM composition different from more luminous systems. We omit the blue dwarfs from the sample to study their effect on the regression results.

T = 0 - 2

T = 3 - 4

T = 5 - 10

